Chiang Mai J. Sci. 2018; 45(5) : 2105-2122
http://epg.science.cmu.ac.th/ejournal/
Contributed Paper

Process Optimization of Biomimetic Calcium Phosphate Coating on 3D Printed Porous Polyethylene by Using Statistical Design of Experiment

Faungchat Thammarakcharoen and Jintamai Suwanprateeb*
National Metal and Materials Technology Center (MTEC), 114 Paholyothin Road, Klong 1, Klongluang, Pathumthani 12120 Thailand.
* Author for correspondence; e-mail: jintamai@mtec.or.th

Received: 1 November 2017
Accepted: 30 April 2018

ABSTRACT

Porous polyethylene has been widely used as implant for both hard and soft tissue replacement since it allowed tissue ingrowth and vascularization within its pores. However, due to its inertness, several studies attempted to improve its bioactivity through surface modification or coating. Biomimetic process which mimics the biological process in nature has been shown to be able to produce bioactive calcium phosphate layer on the surface of biomaterials at low temperature. This process was; thus, applied to create a calcium coating on three dimensionally printed porous polyethylene to possibly increase its bioactivity. Statistical design of experimental methodology based on Taguchi L_{36} design was used to study the effect of various processing parameters on the amount of calcium phosphate coating produced by such technique. The coating process was divided into three main steps and eleven control factors were studied including pretreatment step (pressure, sodium hydroxide concentration, temperature and time), seeding step (pressure, drying method and number of repetition) and coating step (time, temperature, surface to volume ratio and pressure). It was found that pretreatment pressure were the dominant factors with the greatest contribution while pretreatment temperature, seeding pressure, number of seeding repetition, coating time and coating temperature were significant factors. Other control factors had negligible effects on the coating content. For all conditions, plate-like calcium phosphate crystals were similarly found to grow on the surface of 3D printed porous polyethylene, but the crystal size varied. X-ray diffraction revealed that all the coatings consisted of octacalcium phosphate (OCP) and hydroxyapatite (HA) as main phases.

Keywords: calcium phosphate, design of experiment, porous, polyethylene, coating, biomimetic

1. INTRODUCTION

Porous polyethylene has been successfully used in several medical applications such as calvarial reconstruction, ear reconstruction, orbital reconstruction and correction of maxillofacial contour deformities due to its high fracture toughness, ductility and porous structure that could allow tissue in-growth into its pores to provide strong fixation [1-3]. Porous polyethylene is commonly fabricated by sintering process or porogen leaching using mold [4-5], but the shape of samples that were prepared by these techniques were limited to simple-shaped parts due to the nature of indirect molding process which could not match the complexity of anatomical defects. Recently, a direct fabrication of porous polyethylene by three dimensional printing (3D printed porous polyethylene) was developed [6-7]. The advantages of this technique were that the geometries of the implants could be customized to fit the shape of bone defect and the leaching out the porogens from interior part of the implant was not difficult.

For bone replacement application, it is advantageous for the implant to display bioactivity suitable for osteogenesis by forming a biologically active bone-like calcium-phosphate layer on its surface. However, typical polymeric implant generally lacked this property and coating by calcium phosphate layer was frequently employed to alleviate this shortcoming [8-9]. One of the coating processes which has been received interest was the biomimetic process. This coating process mimicked the mineralization process of bone in nature by employing the highly saturated calcium phosphate solution with ions concentration nearly or greater than those of human blood plasma [10-12]. It was considered that this biomimetic coating process could also be adapted to 3D printed porous polyethylene to alter its biological property. In order to achieve an optimal condition for coating process, all involved process parameters which could affect the process performance should be analyzed simultaneously due to the possible interaction among them. However, process parameters in previous works were studied as independent factor or a combination of small numbers of factors. Statistical design of experiment is a powerful tool when the process is influenced by number of parameters. Among several techniques, Taguchi method is frequently employed since it uses orthogonal array and only tests pairs of combinations instead of testing all possible combinations like the full factorial design. Therefore, the numbers of experiments that are needed to be carried out are much lower. This technique has been previously applied to optimize the biomaterials and scaffold fabrication processes [13-14].

In this study, 3D printed porous polyethylene was fabricated and coated by biomimetic process. The effects of process parameters on the biomimetic coating performance were determined by using a statistical design of experiment based on Taguchi orthogonal arrays to analyze the effect of eleven control parameters in the process on the coating content and coating characteristic obtained. Optimal process conditions and the contribution percentage of each parameter were identified. Validation test with the optimal levels of biomimetic coating was also carried out to confirm the effectiveness of this optimization method. In addition, the biocompatibility of the biomimetically calcium phosphate coated 3D printed porous polyethylene was also studied.

2. MATERIALS AND METHODS

2.1 Statistical Design of Experiment

L_{36} mixed level Taguchi orthogonal array with three factors at two levels and eight factors at three levels was employed to evaluate the effects of process parameters in biomimetic calcium phosphate coating on the characteristics and content of coating layer formed on the surface of 3D printed porous polyethylene. Since the biomimetic calcium phosphate coating consisted of three main steps, eleven main factors were studied including pretreatment step (1. pressure, 2. sodium hydroxide concentration, 3. temperature and 4. time), seeding step (5. pressure, 6. drying method and 7. number of repetition) and coating step (8. time, 9. temperature, 10. surface area to solution volume ratio and 11. pressure) as shown in table 1. Thirty six experiments were carried out and the designated main factors and levels in each experiment were shown in tables 2. All experiments were done in triplicate.

Table 1. Studied process factors and levels.

Factor No.	Parameters	Levels of each factor		
		Levels 1	Levels 2	Levels 3
Pretreatment step				
#1	Pretreatment pressure (mbar)	0	Atm	NA
#2	NaOH concentration (M)	1	3	5
#3	Pretreatment temperature (°C)	23	50	70
#4	Pretreatment time (days)	1	2	3
Seeding step				
#5	Seeding pressure (mbar)	0	Atm	NA
#6	Drying pressure at 50 °C (mbar)	Atm	0	NA
#7	Number of repetition (times)	0	4	8
Coating step				
#8	Coating time (h)	2	4	6
#9	Coating temperature (°C)	23	37	50
#10	Surface area to solution volume ratio (mm^2/mL)	20	10	6.67
#11	Coating pressure (mbar)	Atm	500	0

Atm = atmospheric pressure=1,013 mbar.

After all experiments were completed, signal to noise ratio (S/N ratio) and analysis of variance (ANOVA) were determined. In Taguchi method, the quality of the process parameters is assessed by the response of the process main factors to noise and signal. The optimal process conditions would respond to the signals and will be unaffected by noise factors. Therefore, higher values of the signal to noise ratio (S/N ratio) is preferred and used to identify the value of main factors that minimize the influences of the noise factors. In this study, the greater amount of calcium phosphate layer formed on the 3D printed porous polyethylene surface was desired and the coating content would follow the similar trend as that of S/N ratio. Therefore, larger-the-better type of S/N ratio was employed in the analysis using the formulation as following.

$$S/N = -10 \log \sum_{i=1}^{n} \frac{1}{n} \left(\frac{1}{Y_i^2}\right)$$

where n is the number of measurements and Y_i is the measured value

Not only the determination of the process values in each main factors to optimize the process is obtained, analysis of variance (ANOVA) is also commonly applied to the results in Taguchi experiment to determine the contribution percentage of individual main factors to investigate which parameters significantly affected the process. The factor which showed higher contribution percentage will have a greater influence on the performance of the process. The percentage of contribution is a function of the sum of squares for each significant item and can be calculated as:

$$SST = \sum_{i=1}^{n} (n_i - n_m)^2$$

$$SST = \sum_{i=1}^{n} n_i^2 - CF$$

where SST is the total sum of squared deviations

n is the number of experiments in the orthogonal array

n_i is the mean S/N ratio for the i^{th} experiment

n_m is the total mean of S/N ratio

CF is a correction factor

$$SSA = \frac{A_1^2}{N_{A1}} + \frac{A_2^2}{N_{A2}} + ... \frac{A_i^2}{N_{Ai}} - CF$$

where SSA is the sum square of factor A

N_{Ai} is the total number of experiments in which level i on factor A is present

A_i is the total of the results (n_i) that include factor A_i

Four quantities for each factor are then calculated as following:

Mean square or variance

$$(V_a) = \frac{SSA}{DOF_A}$$

$$F \text{ ratio} = \frac{V_a}{V_e}$$

Pure sum of squares (SSAP)

$= SSA-(V_e-DOF_A)$

$$\text{Contribution} = \frac{SSAP}{SST}$$

where DOF_A is the degree of freedom of factor A

V_e is the variance of error which is obtained by calculate error sum of squares and dividing by error degree of freedoms

Table 2. Taguchi L_{36} mixed level orthogonal array.

Experiment	Factors										
No.	#1	#2	#3	#4	#5	#6	#7	#8	#9	#10	#11
1	1	1	1	1	1	1	1	1	1	1	1
2	1	1	2	1	1	1	2	2	2	2	2
3	1	1	3	1	1	1	3	3	3	3	3
4	1	1	1	1	2	2	1	1	2	2	2
5	1	1	2	1	2	2	2	2	3	3	3
6	1	1	3	1	2	2	3	3	1	1	1
7	2	1	1	2	1	2	2	3	1	2	3
8	2	1	2	2	1	2	3	1	2	3	1
9	2	1	3	2	1	2	1	2	3	1	2
10	2	1	1	2	2	1	3	2	1	3	2
11	2	1	2	2	2	1	1	3	2	1	3

Table 2. Continued.

Experiment No.	Factors										
	#1	#2	#3	#4	#5	#6	#7	#8	#9	#10	#11
12	2	1	3	2	2	1	2	1	3	2	1
13	1	2	1	1	1	1	3	1	3	2	1
14	1	2	2	1	1	1	1	2	1	3	2
15	1	2	3	1	1	1	2	3	2	1	3
16	1	2	1	1	2	2	3	2	1	1	3
17	1	2	2	1	2	2	1	3	2	2	1
18	1	2	3	1	2	2	2	1	3	3	2
19	2	2	1	2	1	2	1	3	3	3	1
20	2	2	2	2	1	2	2	1	1	1	2
21	2	2	3	2	1	2	3	2	2	2	3
22	2	2	1	2	2	1	2	3	3	1	2
23	2	3	2	2	2	1	3	1	1	2	3
24	2	3	3	2	2	1	1	2	2	3	1
25	1	3	1	1	1	1	2	1	2	3	3
26	1	3	2	1	1	1	3	2	3	1	1
27	1	3	3	1	1	1	1	3	1	2	2
28	1	3	1	1	2	2	2	2	2	1	1
29	1	3	2	1	2	2	3	3	3	2	2
30	1	3	3	1	2	2	1	1	1	3	3
31	2	3	1	2	1	2	3	3	2	3	2
32	2	3	2	2	1	2	1	1	3	1	3
33	2	3	3	2	1	2	2	2	1	2	1
34	2	3	1	2	2	1	1	2	3	2	3
35	2	3	2	2	2	1	2	3	1	3	1
36	2	3	3	2	2	1	3	1	2	1	2

2.2 3D Printed Porous Polyethylene

High density polyethylene (HDPE) (Thaizex 7000F, Bangkok Polyethylene Co.,Ltd, Thailand) which was grinded and having the mean particle size of approximately 305 microns as determined by a Mastersizer (Malvern (Instruments, UK) was used as a main matrix. The materials used as adhesive binder were maltodextrin (Shandong Duqing, Inc., China) and polyvinyl alcohol (Sigma Aldrich, USA) which were supplied in powder form having particle sizes in the range 80 - 100 μm and used without further sieving. 3D printed porous polyethylene specimens were fabricated by mixing 30% w/w of adhesive binder and 70% w/w of polyethylene powder and loaded in the 3D printing machine (Z400, Z Corporation, USA) to print rectangular specimens (80 mm × 4 mm × 10 mm). After building, all specimens were left in the machine for 2 h before removal and subjected to two-step heat treatment using a wet salt bed technique [8-9]. Briefly, the 3D printed specimens were heated at 145 °C for 1 h, sonicated in deionized water for 24 h and subsequently reheated at 145 °C for 2 h while being covered with sodium chloride powders (Prungtip, Thailand). They were then cleaned in distilled water and dried.

2.3 Biomimetic Calcium Phosphate Coating

Fabricated 3D printed porous polyethylene specimens were cut into rectangular specimens (10 mm × 10 mm × 4 mm) by a sharp blade. They were cleaned in distilled water by ultrasonic bath (Crest CP1100D), dried at 80 °C for 4 h and subjected to biomimetic calcium phosphate coating process by passing through pretreatment step, seeding step and coating step respectively. Pretreatment step was carried out by immersing the specimens in sodium hydroxide (NaOH) solution at specified pressure, concentration, temperature and time. The specimens were then cleaned by deionized water and dried at room temperature. Subsequently, the pretreated specimens were subjected to seeding step by dip-and-dry [15] in previously developed accelerated calcium phosphate solution (ACS) [16] containing Na^+ 154.00 mM, Cl^- 201.70 mM, Ca^{2+} 3.87 mM and HPO_4^{2-} 2.32 mM at designated pressure, drying method and number of repetition. Finally, seeded specimens were subjected to coating step by immersing in ACS solution at specific time, temperature, pressure and surface area to solution volume ratio. All coated specimens were cleaned by distilled water and dried at room temperature.

2.4 Coating Characterizations

Weights of the specimens after and before passing through each step of the biomimetic calcium phosphate coating were measured by a precision balance (Mettler Toledo XS204) and the changes in weight were calculated. Phase composition of the surface of specimens was determined by using X-ray diffractometer (Rigaku TTRAXIII) in thin film mode using a step angle of 0.02 and speed of 5° min^{-1} in the range of 2-35° 2θ. The XRD patterns were compared to JCPDS files to identify the phase composition. Microstructures of the specimens were studied by a scanning electron microscope (JEOL JSM-5410) using an accelerated voltage of 20 kV and a working distance of 20 mm. All specimens were coated by gold sputtering prior to observation. Cell proliferation was analyzed by alamar blue assay. Specimens were placed in the tissue culture 24-well plate and primary human osteoblast suspension (1×10^5 cells per one milliliter) was dripped onto each specimen. They were then incubated at 37 °C with 5% CO_2 and 95% RH. for 3, 7 and 14 days. After incubation at each period, the medium was aspirated and washed. Subsequently, 1 mL of 0.001 % alamar blue solution was added in each well and incubated for 4 h. The optical density of the solution was measured using a spectrophotometer (SpectraMax M5, Molecular Devices, USA) to quantify the cell viability. Reagent control was the well without specimens and all experiments were run in triplicate.

2.5 Statistical Analysis

The significant differences in properties among samples were analyzed using an analysis of variance (ANOVA) and Tukey post hoc testing. A value of $p < 0.05$ was considered significant.

3. RESULTS

3.1 Calcium Phosphate Coating Characteristics

3.1.1 Weight change

Table 3 shows the weight change of the specimens after passing through each step. Pretreatment step generally resulted in the decrease in weight of specimens. However, some slight increases in the weight were also seen in some specimens. In the case of seeding and coating steps, weight of the all

specimens increased, but the content depended on the conditions used. Low (below 0.5 mg), medium (0.5-1.0 mg) and high (above 1.0 mg) content in weight change were employed as criteria for examination. Experiment numbers 10, 16, 18, 23, 24, 25, 29, 30, 34 and 36 gave high weight change in seeding step while the high weight change in coating step was gained in experiment numbers 3, 5, 13, 15, 19, 22, 25, 26, 29 and 31. Medium weight change was seen in experiment numbers 6, 11, 12, 17, 22, 31 and 35 in seeding step and experiment numbers 2, 4, 6, 7, 9, 10, 16, 21, 23, 27 and 28 in coating step. Others experiment numbers gave low weight changes. Considering the total weight change, experiment number 29 showed the greatest value.

Table 3. Weight change, phase composition and coating morphology/structure in each experiment (n=3).

Experiment No.	Weight change (mg)				Phase	Coating morphology and structure
	Pretreatment step	Seeding step	Coating step	Total		
1	-0.07±0.12	0.03±0.06	0.50±0.20	0.46±0.10	HA	S, P
2	-0.33±0.25	0.13±0.25	0.87±0.21	0.67±0.21	OCP, HA	S, P
3	-0.13±0.06	0.13±0.15	1.43±0.15	1.43±0.21	OCP, HA	P
4	-0.07±0.15	0.10±0.00	0.87±0.38	0.90±0.15	HA	S, I, P
5	-0.07±0.25	0.50±0.26	1.47±0.67	1.90±0.36	OCP, HA	P
6	-0.40±0.26	0.87±0.15	0.80±0.17	1.27±0.32	HA	P
7	0.00±0.20	0.27±0.15	0.77±0.21	1.04±0.06	HA	S, P
8	-0.40±0.10	0.43±0.21	0.33±0.15	0.36±0.31	HA	S, P
9	-0.53±0.06	0.30±0.00	0.73±0.25	0.50±0.17	OCP, HA	S, P
10	-0.07±0.21	1.30±0.20	0.57±0.12	1.80±0.10	HA	P
11	0.60±1.05	0.65±0.07	0.20±0.00	1.45±0.49	OCP, HA	S, P
12	-0.17±0.40	0.80±0.00	0.20±0.00	0.83±0.17	OCP, HA	P
13	-0.30±0.10	0.40±0.17	1.03±0.40	1.13±0.32	OCP, HA	P
14	-0.63±0.21	0.50±0.26	0.37±0.21	0.24±0.31	HA	S, P
15	-0.27±0.15	0.15±0.07	1.13±0.15	1.01±0.35	HA	P
16	0.10±0.10	1.13±0.55	0.53±0.50	1.76±0.15	HA	S, P
17	-0.37±0.23	0.67±0.25	0.25±0.07	0.55±0.17	HA	S, I
18	-0.40±0.36	1.03±0.32	0.40±0.26	1.03±0.25	OCP, HA	G
19	0.10±0.26	0.25±0.21	1.43±0.15	1.78±0.10	OCP, HA	S, I
20	-0.33±0.21	0.27±0.21	0.30±0.26	0.24±0.06	HA	S
21	0.13±0.23	0.10±0.14	0.83±0.12	1.06±0.10	HA	S, P
22	0.23±0.15	0.57±0.55	1.00±0.26	1.80±0.20	OCP, HA	I
23	0.03±0.32	1.13±0.40	0.60±0.20	1.76±0.15	HA	P
24	-0.17±0.06	1.53±0.67	-0.50±0.00	0.86±0.21	HA	S, I
25	-0.20±0.20	1.30±0.99	-0.30±0.00	0.80±0.25	HA	S, I
26	-0.17±0.31	0.10±0.00	1.33±0.35	1.26±0.36	OCP, HA	S, P
27	-0.60±0.20	0.33±0.47	0.57±0.15	0.30±0.46	HA	S, P
28	-0.20±0.20	0.47±0.15	0.60±0.20	0.87±0.21	OCP, HA	P

Table 3. Continued.

Experiment No.	Weight change (mg)				Phase	Coating morphology and structure
	Pretreatment step	Seeding step	Coating step	Total		
29	0.37±0.25	1.03±0.15	1.73±0.42	2.39±0.40	OCP, HA	P
30	-0.50±0.00	2.00±0.84	-0.67±0.00	0.83±0.10	HA	S
31	-0.07±0.06	0.73±0.68	1.63±0.31	1.29±0.72	OCP, HA	S, P
32	0.13±0.12	0.10±0.00	0.47±0.32	0.70±0.06	HA	S
33	-0.07±0.12	0.05±0.07	0.13±0.12	0.11±0.10	Not detected	N.A.
34	-0.17±0.15	1.10±0.57	0.50±0.28	1.43±0.06	HA	S, G
35	0.07±0.38	0.80±0.20	0.13±0.15	1.00±0.17	HA	S, P
36	-0.17±0.06	1.40±0.20	0.30±0.10	1.53±0.23	HA	P

Note: S=Smooth layer; G=Globular structure, I=Isolated spheroids of plate-like crystals; P=Uniform interconnected plate-like crystals vertically grown on the surface.

3.1.2 Phase composition

Typical XRD patterns of the coated surfaces after passing through biomimetic calcium phosphate coating were shown in figure 1. Two types of calcium phosphate were mainly found on the surfaces of specimens including octacalcium phosphate (OCP) and hydroxyapatite (HA). This was indicated by main characteristic peaks of OCP at 2θ degrees of 4.7, 9.4 and 9.7 (JCPDS card # 26-1056) and the peaks at 2θ degrees of 26 and 31.0-34.1 which could be assigned to OCP (JCPDS card # 26-1056) or HA (JCPDS card # 09-432) since they are generally overlapped. The intensity of these peaks varied depending on the experimental conditions and the phase compositions of the specimens in each experiment were summarized in table 3. However, no calcium phosphate peaks could be detected in experiment number 33 and only characteristic peaks of polyethylene were seen.

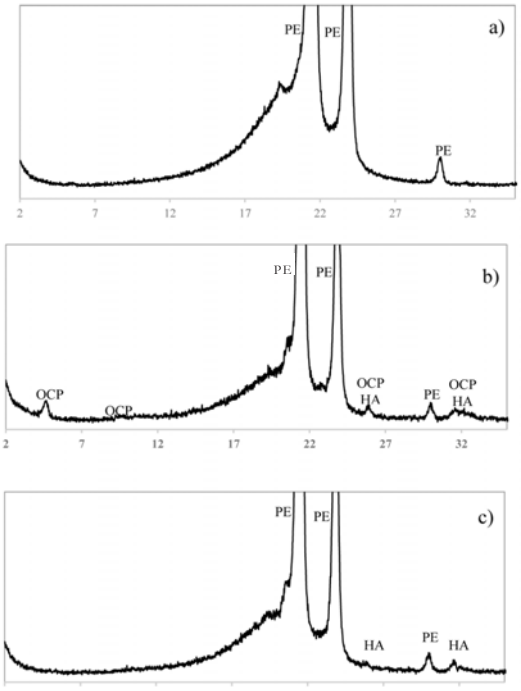

Figure 1. Typical XRD patterns of the surface of the samples after passing through biomimetic coating process; a) HDPE or Not detected (experiment number 33); b) OCP, HA (experiment number 29) and c) HA (experiment number 35).

3.1.3 Morphology and microstructure

Figure 2 shows the microstructure of 3D printed porous polyethylene which was used as substrate in this study. Particle bridging structures with numerous pores as a result of heat treatment were observed. At high magnification, the surface of the specimen appeared smooth and minute polyethylene crystal morphology could also be seen. Figure 3 shows the effect of process parameters on coating microstructure in each experiment number as designed by Taguchi method. No coating was produced in experiment number 33 indicating that this condition was not appropriate for biomimetic coating on 3D printed porous polyethylene. For other experiment numbers, coating was successfully produced on the surface of 3D printed porous polyethylene. Generally, four main types of coating morphology and structures were observed depending on the process conditions used including smooth layer, globular structure, isolated spheroids of plate-like crystals and uniform interconnected plate-like crystals vertically grown on the surface. It should be noted that more than one type of morphology and structure could be obtained in one specimen. In the case of plate-like crystal morphology, the size and maturity of crystals also varied with process conditions for example in experiment numbers 23, 27 and 35 where crystals only started to grow compared to the highly grown crystals in experiment numbers 3, 5, 12, 13, 28, 29. Table 3 summarized the type of crystal morphology and structure of the coating found on the surface of specimen in each experiment number.

3.2 Process Optimization

Figure 4 shows the plot of calculated S/N ratio and eleven main factors used in this study. From the plot, the maximum values of S/N ratio for each main factors were identified and the optimal conditions for biomimetic calcium phosphate coating on 3D printed porous polyethylene was; thus, obtained as shown in table 4. Results of ANOVA analysis in table 5 also indicated that pretreatment pressure was a dominant factor for coating process with the greatest contribution (22.2%) while pretreatment temperature (12.7%), seeding pressure (10.8%), number of seeding repetition (13.6%), coating time (17.8%) and coating temperature (7.0%) were significant factors with lower contributions. Other factors had negligible effect on coating process.

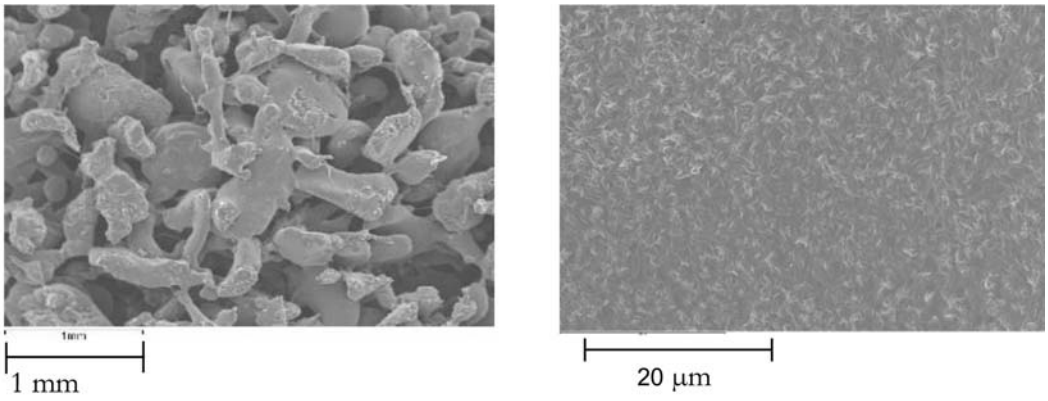

Figure 2. SEM images showing the microstructure of 3D printed porous polyethylene.

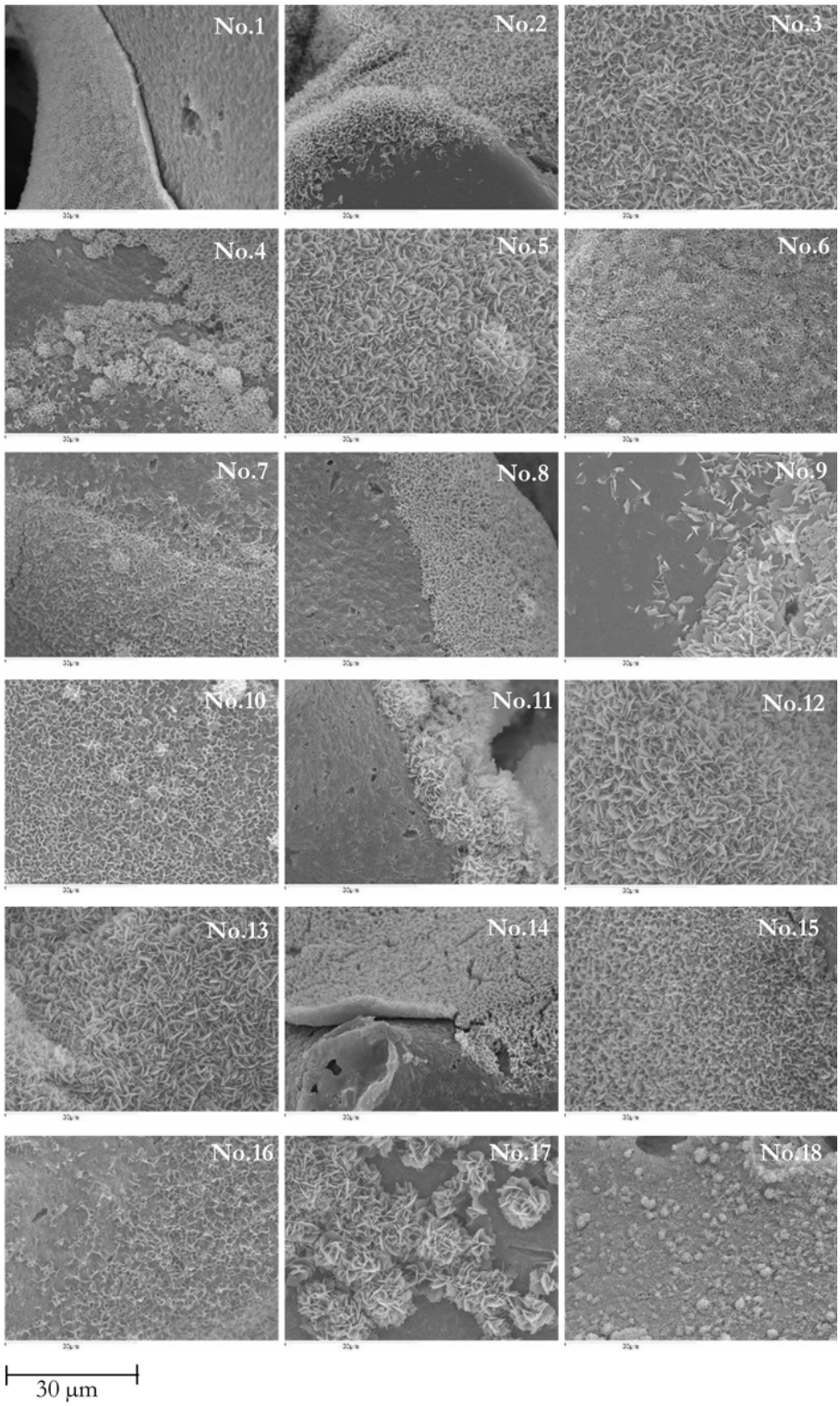

Figure 3. SEM images showing the microstructure of coated 3D printed porous polyethylene produced by biomimetic process in each experiment in Taguchi analysis.

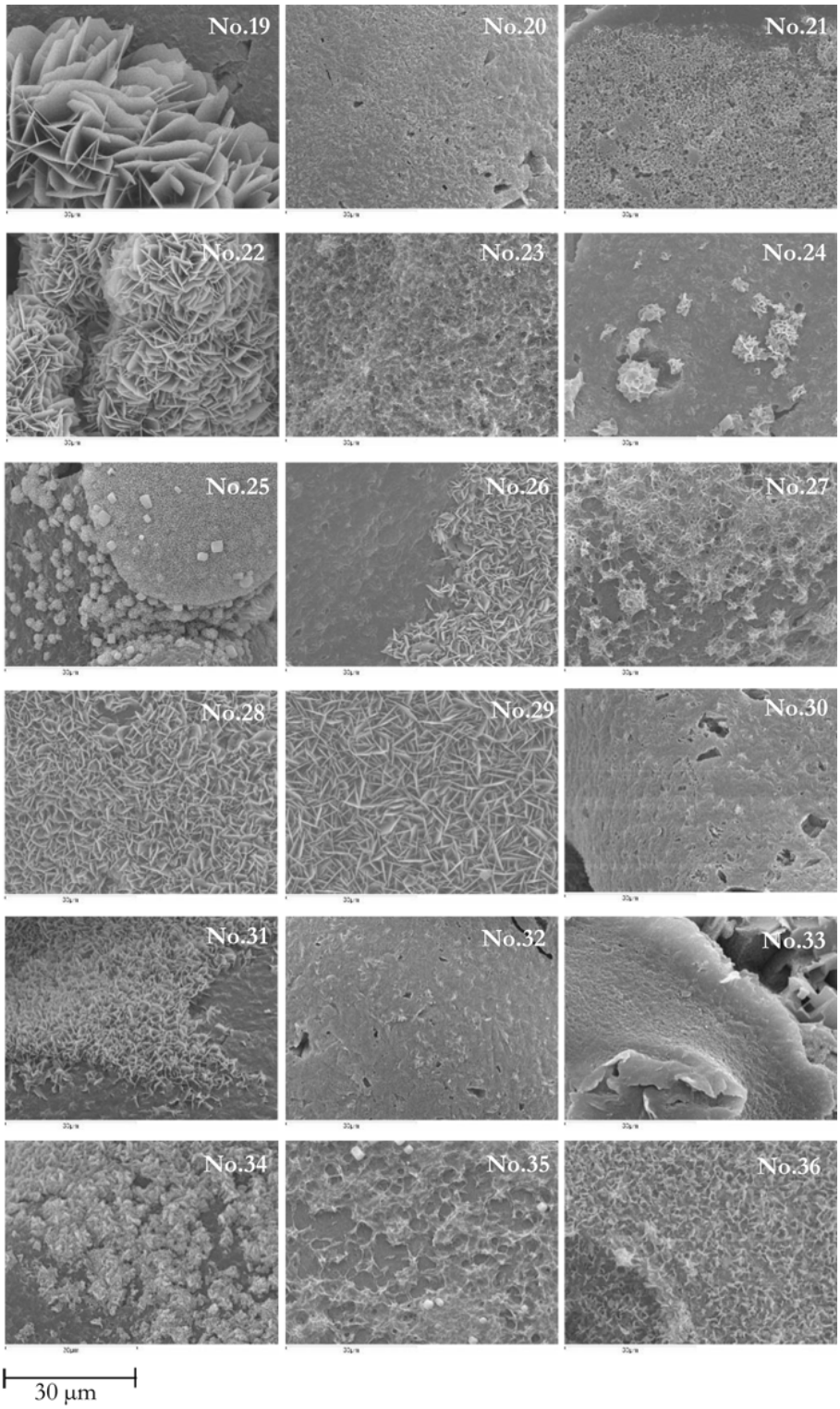

Figure 3. SEM images showing the microstructure of coated porous polyethylene produced by biomimetic process in each experiment in Taguchi analysis (cont).

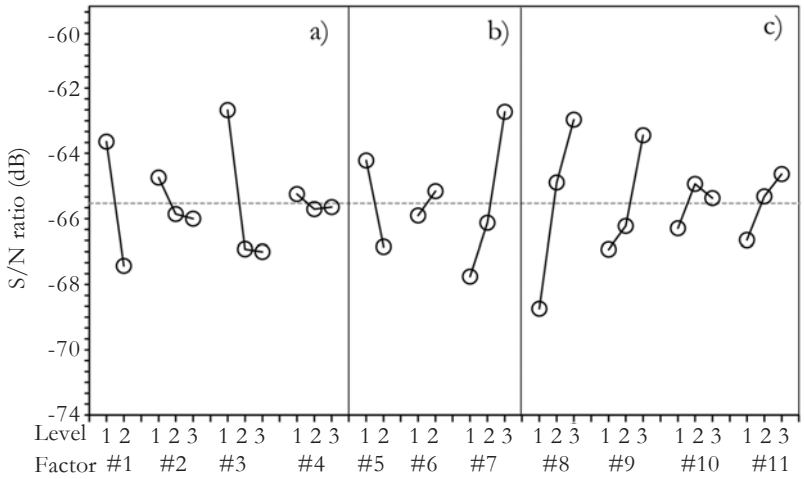

Figure 4. Influence of process parameters on S/N ratio; a) pretreatment step, b) seeding step and c) coating step.

Table 4. Optimum process parameters for maximum weight change obtained from S/N ratio analysis.

Factor No.	Parameters	Values
Pretreatment step		
#1	Pretreatment pressure (mbar)	0
#2	NaOH concentration (M)	1
#3	Pretreatment temperature (°C)	23
#4	Pretreatment time (days)	1
Seeding step		
#5	Seeding pressure (mbar)	0
#6	Drying pressure at 50 °C (mbar)	0
#7	Number of repetition (times)	8
Coating step		
#8	Coating time (h)	6
#9	Coating temperature (°C)	50
#10	Surface area to solution volume ratio (mm^2/mL)	10
#11	Coating pressure (mbar)	0

Table 5. ANOVA table for analyzing the effect of process parameters on weight change.

Factor No.	Parameters	Degree of freedom	Sum of square	Mean square	F	Contribution (%)
Pretreatment step						
#1	Pretreatment pressure (mbar)	1	186.3	186.3	13.6	22.2
#2	NaOH concentration (M)	2	16.5	8.3		1
#3	Pretreatment temperature (°C)	2	212.2	106.1	7.8	12.7
#4	Pretreatment time (days)	2	2.2	1.1		0.1
Seeding step						
#5	Seeding pressure (mbar)	1	90.1	90.1	6.6	10.8
#6	Drying pressure at 50 °C (mbar)	1	7.3	7.3		0.9
#7	Number of repetition (times)	2	227.6	113.8	8.3	13.6
Coating step						
#8	Coating time (h)	2	298.7	149.3	10.9	17.8
#9	Coating temperature (°C)	2	117	58.5	4.3	7
#10	Surface area to solution volume ratio (mm^2/mL)	2	16.7	8.4		1
#11	Coating pressure (mbar)	2	32.5	18.3	1.3	2.2
	Error					10.8
	Total					100

In order to see if Taguchi method could well predict the optimal coating conditions, the validated experiment was further carried out by preparing specimens according to the optimal process condition as shown in table 4 and characterized. The weight change of validated specimens gave the total weight change ranging between 1.70-2.30 mg and the phase composition comprised the mixture of OCP and HA. Coating morphology was observed to be uniform and distributed interconnected plate-like crystals vertically grown on the surface of 3D printed porous polyethylene (figure 5a). Figure 5b shows the osteoblast proliferation on the surface of uncoated and biomimetic coated 3D printed porous polyethylene using optimal conditions. Both samples supported the osteoblast growth on the surfaces since the optical density of alamar blue increased with increasing incubation periods. Coated sample had slightly lower cell proliferations than those of uncoated sample, but the difference was not statistically significant ($p > 0.05$).

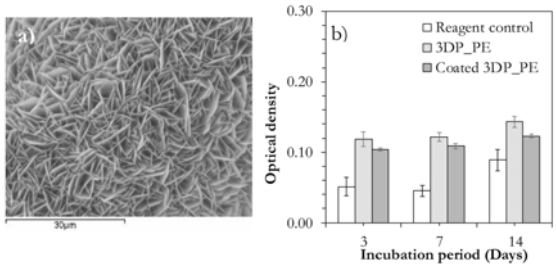

Figure 5 Biomimetically calcium phosphate coated 3D printed porous polyethylene using optimal conditions as predicted by Taguchi method; a) Morphology and microstructure and b) Osteoblast proliferation (n=3).

4. DISCUSSION

The biomimetic calcium phosphate process used in this study comprised three main steps including pretreatment step, seeding step and coating step. In typical biomimetic coating process, pretreatment step was crucial and was done prior to the coating step to produce the appropriate surface suitable for crystallization of calcium phosphate crystals to start rapidly when the surface was in contact with highly saturated calcium phosphate solution. Since hydrophobic polyethylene has typical low chemical reactivity surface due to its apolar nature, pretreatment step in this study was done to enhance the hydrophilicity of polyethylene surface which would be more suitable for calcium phosphate nucleation to initiate. Several surface modification techniques for polymers have been reported previously including ion beam process, oxygen cluster beam irradiation, ultraviolet irradiation, glow discharge and hydrogen peroxide treatment [17-18]. In this study, alkali treatment by NaOH was chosen since the condition was milder and simpler, but still provided the effective result [19-20]. Surface etching and hydrolysis were the main outcomes of this alkali pretreatment. Slight weight change and even the decrease in weight of the sample after passing through this step were expected. This corresponded well to the weight change results in table 3 which mostly decreased for all experiment numbers.

Following the pretreatment step, seeding step was devised to pre-deposit the calcium phosphate nuclei or even the primary crystals to induce and accelerate the crystal initiation and growth on the surface of non-active 3D printed porous polyethylene. It was reported that the calcium phosphate nuclei formed on the metallic surface by repeating the dip-and-dry treatment could readily grow to calcium phosphate coating when being immersed in the supersaturated solution [15]. The use of sodium silicate solution to induce apatite nuclei on the surface of polyethylene terephthalate was reported to be a vital step for the formation of continuous apatite layer after soaking in 1.5 simulated body fluid [21-22]. Without this step, no apatite layer was formed on the polymer surface. In this study, accelerated calcium phosphate solution (ACS) was employed for this purpose. It was developed and shown previously that ACS could induce the formation of calcium phosphate layer on the metallic surface much faster than the typical use of simulated body fluid [16]. From weight change measurement in this study, all experiment numbers displayed the increase in weight of the specimens after passing through this seeding step. The weight change, presumably the content of pre-deposited calcium phosphate nuclei or crystals, was observed to increase with the increase in number of seeding repetition and the use of vacuum condition during seeding. It was rather obvious that increasing number of seeding would deposit more calcium phosphate nuclei or crystal on the surface. Due to the porous structure of 3D printed porous polyethylene, vacuum helped to drive the ACS solution to flow through the pores to reach the inner part and interact with the whole surface of the specimens.

After passing through the coating step, weight of the specimens further increased compared to those of seeding step. This obviously indicated that the coating was successfully produced on the surface of 3D printed porous polyethylene. The weight change in coating step tended to increase with the increase in coating time and temperature and corresponded well to the coating microstructure as observed by SEM. Continuous and large amount of coating were found on the surface of specimens

which showed high weight change. From SEM analysis, several morphologies and microstructures of calcium phosphate coating formed on the surface of 3D printed porous polyethylene were observed and could be categorized into four main types including smooth layer, globular structure, isolated spheroids of plate-like crystals and uniform interconnected plate-like crystals vertically grown on the surface. Among these, both isolated and uniform plate-like structures were generally observed in coating layer formed by biomimetic coating using simulated body fluid [8, 23-24]. It was also thought that the crystal maturity due to the growth increased from smooth layer to plate-like morphology since the specimens with high weight changes generally displayed uniform interconnected plate-like crystal structure. Since biomimetic coating relied on the crystallization under supersaturation conditions, there always be a competition between crystal nucleation and crystal growth which ultimately determined the final crystal microstructure. Temperature generally affected both nucleation and crystal growth by manipulating the solubility of the sample and supersaturation of solution [25] while coating time would primarily influence the crystal growth process. The process conditions that favored the crystal nucleation would produce large numbers of nuclei and ultimately resulted in smaller, but larger number of crystals (for examples in experiment numbers 3, 28 and 29). In contrast, process conditions that preferred crystal growth would produce lower numbers of nuclei and resulted in more isolated, but larger crystals (for example in experiment numbers 19 and 22). In the case of phase composition, the intensity of XRD patterns increased with the increase in the weight change of the specimens which was presumably the coating content. OCP and HA were identified as main phases in the coating. In the case of experiment number 33, no calcium phosphate pattern was detected. This could be either the coating was not formed or the content was too low to be detected by XRD technique. From SEM observation, no distinct coating was observed and the weight change of this specimen was also limited. No clear influence of the weight change and coating microstructure on the phase of the coating was observed. This was possibly due to the closed similarity of OCP and HA. OCP was sometimes regarded as a precursor of HA and could convert to HA readily due to their mineralogical correlation [26-27].

From process analysis point of view, only pretreatment pressure, pretreatment temperature, seeding pressure, number of seeding repetition, coating time and coating temperature should be considered since they significantly contributed to the performance of coating process. It was seen that S/N ratios decreased with increasing pretreatment temperature, but increased with the increase in seeding repetition, coating time and coating temperature. S/N ratios were relatively unchanged with NaOH concentration, pretreatment time or surface area to solution ratio. Since pretreatment step etched the surface of the sample resulting in the removal of materials as seen by the decrease in weight change in pretreatment step, the increase in pretreatment temperature might accelerate the etching process and negatively affected the S/N ratio. Although it was previously reported that increasing NaOH concentration could induce faster apatite formation on the surface of polyether ether ketone and polyethylene [20], NaOH concentration or pretreatment time did not show significant influence in this study. Previous study relied on the NaOH pretreatment only to induce the apatite

formation while both NaOH pretreatment and calcium phosphate seeding were employed in current study. Thus, the importance of alkali pretreatment in this study might be reduced. In addition, it should be noted that this study evaluated the effect of such pretreatment parameters on the whole calcium phosphate coating formation. Therefore, the correlation between the content of coating and the pretreatment parameters might not follow the same direction and could be influenced by the interaction among process parameters. This is the advantage of Taguchi method when studying the process which is influenced by several parameters simultaneously. In the case of number of seeding repetition, coating time and coating temperature, it was logical that all these factors positively affect S/N ratio since they all resulted in the crystal growth and coating formation. For pretreatment and seeding pressure, the use of vacuum (0 mbar) was shown to similarly increase the S/N ratio. This was obviously related to the complicated structure of 3D printed porous polyethylene which needed the help to drive the NaOH solution or ACS solution to flow deep into the pores to interact with the whole surface of the samples as discussed previously.

Generally, the final step of Taguchi design is to validate the prediction by experimentation. In the validated experiment in this study, the total weight change of the optimal condition specimens was greater than those of 36 experiments. It was also comparable and not significantly difference to the content obtained from experiment no. 29 which was the best condition in 36 experiments. The differences between these two conditions were pretreatment NaOH concentration, pretreatment temperature, seeding pressure and coating pressure. Among these, only pretreatment temperature and seeding pressure were significant factors while pretreatment NaOH concentration and coating pressure were negligible effects according to ANOVA analysis. However, these two significant factors contributed to only 10.8 % and 13.6 % respectively for the whole process and might not cause much difference. Therefore, the robustness of Taguchi method in predicting the optimal biomimetic calcium phosphate coating process parameters were proven and validated. Compared to other surface coating studies which were done on flat and nonporous surface and involved relatively low number of factors [28-29], the porous and interconnected structure of 3D printed porous polyethylene and eleven main factors used in this study were more challenged to analyze and predict the efficient coating process. However, it is typical for statistical process optimization that the process could be repeated more than once. Further optimization of biomimetic coating on 3D printed porous polyethylene could also be carried out to include other parameters and targets for example cleaning method, the surface coverage percentage and coating thickness or the use of combined target approach.

In the case of biocompatibility, alamar blue assay revealed that both uncoated and coated samples were nontoxic and were sufficiently biocompatible for osteoblasts to grow on. However, coated sample displayed slightly lower cells proliferation than those of uncoated sample. Previously, lower osteoblast proliferation of biomimetically coated polycarbonate urethane than that of uncoated sample was also reported and was attributed to the dissolution of coating over time [12]. This could be the possible cause for lower optical density of coated sample compared to uncoated sample seen in this study as well. However, it should be noted that the

difference was not statistically significant ($p>0.05$) and the cell proliferations of both samples were still significantly greater ($p< 0.05$) than those of the reagent control. However, further study could be carried out to investigate the underlying causes.

5. CONCLUSIONS

The surface of 3D printed porous polyethylene was successfully coated by calcium phosphate layer by using biomimetic process. Octacalcium phosphate and hydroxyapatite were found to be the main phases of the coating. Taguchi robust design of experiment was able to effectively identify the contribution percentage of the process parameters on the calcium phosphate coating content and the corresponding optimal process conditions. Validated experiment showed that the prediction was in good agreement with the experimental results. However, future studies are still needed by further including more parameters or targets in the optimization to increase the efficiency of the biomimetic coating process.

ACKNOWLEDGEMENTS

Platform Technology Program, National Metal and Materials Technology Center (MTEC) is thanked for financial support. W. Chokevivat is acknowledged for help in biocompatibility test.

REFERENCES

[1] Wellisz V., *Aesthetic Plast. Surg.*, 1993; **17**: 339-344. DOI 10.1007/bf00437109.

[2] Liu J.K., Gottfried O.N., Cole C.D., Dougherty W.R. and Couldwell W.T., *Neurosurg. Focus*, 2004; **16(3)**: 1-5. DOI 10.3171/foc.2004.16.3.14.

[3] Yaremchuk M.J., *Plast. Reconstr. Surg.*, 2003; **111**: 1818-1827. DOI 10.1097/01.prs.0000056866.80665.7a.

[4] Pal K., Bag S. and Pal S., *J. Porous Mater.*, 2008; **15**: 53-59. DOI 10.1007/s10934-006-9051-9.

[5] Kwon J.H., Kim S.S., Kim B.S., Sung W.J., Lee S.H., Lim J.I., Jung Y., Kim S.H., Kim S.H. and Kim Y.H., *J. Bioact. Compat. Polym.*, 2005; **20(4)**: 361-376. DOI 10.1177/0883911505055386.

[6] Suwanprateeb J., Thammarakcharoen F., Wongsuvan V. and Chokevivat W., *J. Porous Mater.*, 2011; **19(5)**: 623-632. DOI 10.1007/s10 934-011-9513-6.

[7] Suwanprateeb J., Thammarakcharoen F. and Suvannapruk W., *Chiang Mai J. Sci.*, 2014; **41(1)**: 200-212.

[8] Oliveira A.L., Malafaya P.B. and Reis R.L., *Biomaterials*, 2003; **24**: 2575-2584. DOI 10.1016/s0142-9612(03)00060-7.

[9] Miyaji F., Kim H.M., Handa S., Kokubo T. and Nakamura T., *Biomaterials*, 1999; **20**: 913-919. DOI 10.1016/s0142-9612 (98)00235-x.

[10] Lluch A.V., Ferrer G.G. and Pradas M.M., *Polymer*, 2009; **50**: 2874-2884. DOI 10.1016/j.polymer.2009.04.022.

[11] Aparecida A.H., Fook M.V.L. and Guastaldi A.C., *J. Mater. Sci.-Mater. M.*, 2009; **20**: 1215-1222. DOI 10.1007/s10856-008-3682-0.

[12] Barnes D.H., Cameron R.E., Kiamil S., Meyer F., Brooks R.A., Rushton N. and Best S.M., *Bioceram. Dev. Appl.*, 2011; **1**: 1-4. DOI 10.4303/bda/d101111.

[13] Ajaal T.T. and Smith R.W., *J. Mater. Process. Technol.*, 2009; **209**: 1521-1532. DOI 10.1016/j.jmatprotec.2008.04.001.

[14] Fallahiarezoudar E., Ahmadipourroudposht M., Idris A. and Yusof N.M., *Mater. Sci. Eng. C.*, 2017; **76**: 616-627. DOI 10.1016/j.msec.2017.03.120.

[15] Duan K., Tang A. and Wang R., *Mater. Sci. Eng. C*, 2009; **29**: 1334-1337. DOI 10.1016/j.msec.2008.10.028.

[16] Thammarakcharoen F., Suvannapruk W. and Suwanprateeb J., *J. Nanosci. Nanotechnol.*, 2014; **14**: 1-7. DOI 10.1166/jnn.2014.9569.

[17] Baker K.C., Drelich J., Miskioglu I., Israel R. and Herkowitz H.N., *Acta Biomater.*, 2007; **3**: 391-401. DOI 10.1016/j.actbio.2006.08.008.

[18] Kim H.M., Uenoyama M., Kokubo T., Minoda M., Miyamoto T. and Nakamura T., *Biomaterials*, 2001; **22**: 2489-2494. DOI 10.1016/s0142-9612(00)00437-3.

[19] Tanahashi M., Yao T., Kokubo T., Minoda M., Miyamoto T., Nakamura T. and Yamamuro T., *J. Appl. Biomater.*, 1994; **5**: 339-347. DOI 10.1002/jab.770050409.

[20] Pino M., Stingelin N. and Tanner K.E., *Acta Biomater.*, 2008; **4**: 1827-1836. DOI 10.1016/j.actbio.2008.05.004.

[21] Tanahashi M., Yao T. and Kokubo T., *J. Am. Ceram. Soc.*, 1994; **77**: 2805-2508. DOI 10.1111/j.1151-2916.1994.tb04508.x.

[22] Miyaji F., Kim H.M., Handa S., Kokubo T. and Nakamura T., *Biomaterials*, 1999; **20**: 913-919. DOI 10.1016/s0142-9612(98)00235-x.

[23] Kokubo T. and Takadama H., *Biomaterials*, 2006; **27**: 2907-15. DOI 10.1016/j.biomaterials.2006.01.017.

[24] Kawai T., Ohtsuki C., Kamitakahara M., Hosoya K., Tanihara M., Miyazaki T., Sakaguchi Y. and Konagaya S., *J. Mater. Sci.-Mater. M.*, 2007; **18**: 1037-1042. DOI 10.1007/s10856-006-0081-2.

[25] Judge R.A., Jacobs R.S., Frazier T., Snell E.H. and Pusey M.L., *Biophys. J.*, 1999; **77**: 1585-1593. DOI 10.1016/s0006-3495(99)77006-2.

[26] Ito N., Kamitakahara M., Yoshimura M. and Ioku K., *Mater. Sci. Eng. C.*, 2014; **40**: 121-126. DOI 10.1016/j.msec.2014.03.034.

[27] Suzuki O., *Jpn. Dent. Sci. Rev.*, 2013; **49**: 58-71. DOI 10.1016/j.jdsr.2013.01.001.

[28] Das S.K. and Sahoo P., *Tribol. Ind.*, 2010; **32**: 17-27. Retrieved from http://www.tribology.fink.rs/

[29] Winnicki M., Malachowska A. and Ambroziak A., *Arch. Civ. Mech. Eng.*, 2014; **14**: 561-568. DOI 10.1016/j.acme.2014.04.006.